Dependence of Protein-induced Lipid Bilayer Thickness Deformations on Protein Shape

Carlos D. Alas and Christoph A. Haselwandter

Department of Physics & Astronomy and Department of Quantitative & Computational Biology,
University of Southern California, Los Angeles, CA 90089, USA

Abstract

Structural biology has shown that membrane proteins come in a great variety of shapes, with distinct membrane proteins, and even different conformational states of the same membrane protein, often showing distinct hydrophobic thicknesses deviating from the unperturbed thickness of the surrounding lipid bilayer. The resulting protein-induced bilayer thickness deformations can be captured quantitatively by membrane elasticity theory, and have been found to play an important role in membrane protein regulation. Physical models of protein-induced bilayer thickness deformations usually focus on idealized, cylindrical membrane protein shapes. We describe here a boundary value method for the straightforward calculation of protein-induced bilayer thickness deformations for arbitrary protein shapes. We find that the deviations of protein shape from rotational symmetry suggested by structural biology can have a significant effect on the energy of protein-induced bilayer thickness deformations. Intriguingly, our calculations suggest that the elastic coupling of lipid bilayer properties and membrane protein conformational state may provide a generic physical mechanism for temperature sensing through ion channels.

Why care about protein shape?

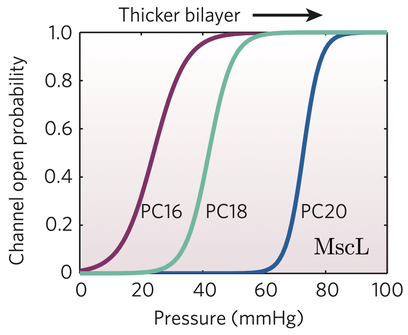

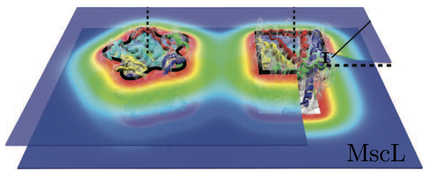

- Protein function depends on bilayer thickness. E.g., MscL [1] is less likely to respond to changes in osmotic pressure in thicker bilayers [2, 3].
- Proteins can have distinct shapes (and can change shape), which induce distinct bilayer deformations [4].
- Historically, energy calculations usually assumed rotational symmetry of the protein.

Bilayer thickness deformation field and energy model

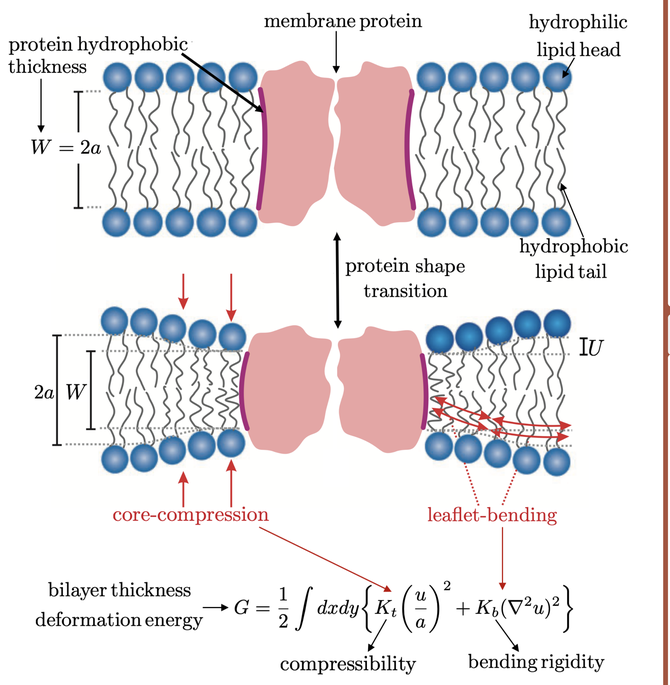

- Amphiphilic interactions and dissimilar hydrophobic thicknesses between proteins and lipid bilayer result in short ranged (decay length $\lambda \sim 1$ nm) local bilayer thickness deformations u [5].
- Standard membrane elasticity theory describes the energetic cost of small u [6].
- Deformation parameters K_t and K_b can be measured by micropipette experiments.
- In static equilibrium, G is minimized by u of form:

$$u(r,\theta) = f^+(r,\theta) + f^-(r,\theta),$$
$$f^\pm(r,\theta) = A_0^\pm K_0\left(\sqrt{\pm\mathbf{i}}\, r/\lambda\right) + \sum_{n=1}^{\infty}\left[A_n^\pm \cos(n\theta) + B_n^\pm \sin(n\theta)\right] K_n\left(\sqrt{\pm\mathbf{i}}\, r/\lambda\right)$$

where K_n are modified Bessel functions of second kind and coefficients $A_n^\pm$ and $B_n^\pm$ are set by protein-lipid interactions [7].

Modeling protein shape and protein-lipid interactions

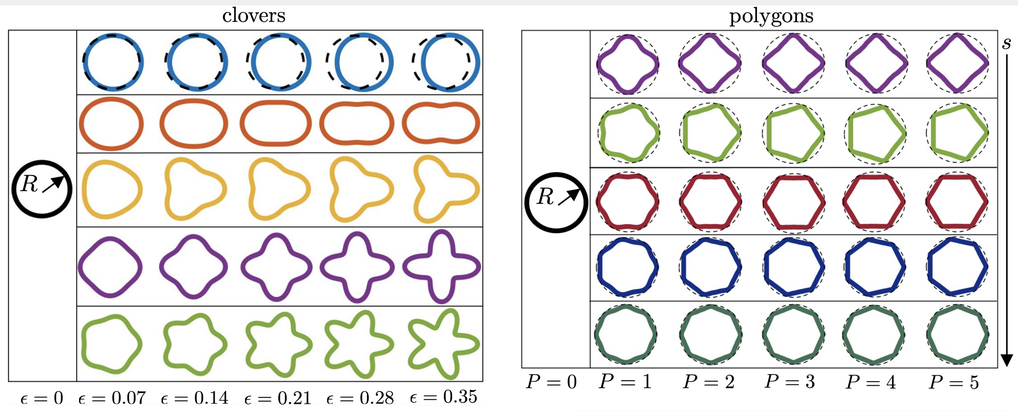

$$C_{\mathrm{clover}}(\theta) = [1 + \epsilon\cos(s\theta)]\, R$$

$$A_R = \frac{R}{\sum_{p=-P}^{P}\frac{1}{(sp+1)^2}} \qquad C_{\mathrm{polygon}}(\theta) = A_R\sqrt{\left[\sum_{p=-P}^{P}\frac{\cos(sp+1)\theta}{(sp+1)^2}\right] + \left[\sum_{p=-P}^{P}\frac{\sin(sp+1)\theta}{(sp+1)^2}\right]}$$

- To demonstrate our methodology, we modeled proteins with clover-leaf and polygon [8] cross-sections, roughly inspired by MscL.
- Bilayer deforms in hydrophobic thickness locally to match protein's hydrophobic thickness at boundary:

Perfect hydrophobic thickness matching boundary condition $\rightarrow u(r,\theta)|_{r=C(\theta)} = U(\theta), \qquad U(\theta) = [W(\theta) - 2a]/2$

Clamped contact slope boundary condition $\rightarrow \hat{\mathbf{n}}\cdot\nabla u(r,\theta)|_{r=C(\theta)} = U'(\theta)$, $\hat{\mathbf{n}}$ = boundary curve unit normal; points into the protein

Numerical boundary value method (BVM) for bilayer thickness deformations due to protein of arbitrary shape

Bilayer thickness deformation field u truncated to finite number of terms N for a desired accuracy in deformation energy G:

$$u(r,\theta) \approx f_N^+(r,\theta) + f_N^-(r,\theta), \qquad f_N^\pm(r,\theta) = A_0^\pm K_0\left(\sqrt{\pm\mathbf{i}}\, r/\lambda\right) + \sum_{n=1}^{N}\left[A_n^\pm \cos(n\theta) + B_n^\pm \sin(n\theta)\right] K_n\left(\sqrt{\pm\mathbf{i}}\, r/\lambda\right)$$

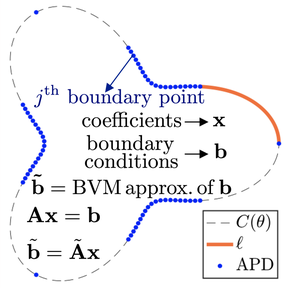

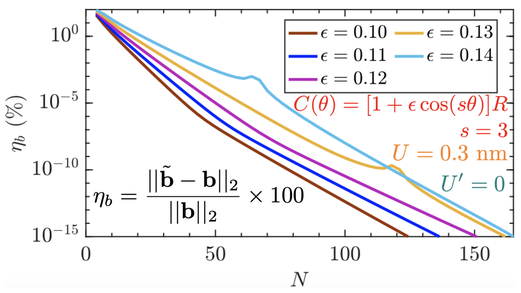

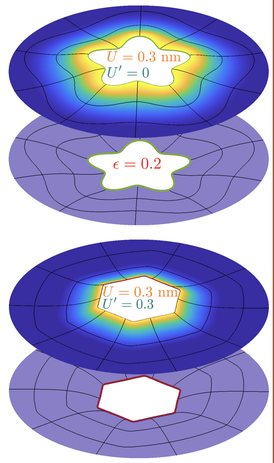

- Coefficients $A_n^\pm$ and $B_n^\pm$ fixed by boundary conditions at $2N+1$ points on boundary:

$$u(r,\theta_j)|_{r=C(\theta_j)} = U(\theta_j),$$
$$\hat{\mathbf{n}}\cdot\nabla u(r,\theta_j)|_{r=C(\theta_j)} = U'(\theta_j)$$

- Adaptive point distributions (APDs) dramatically boost BVM convergence rates with denser set of evaluation points along negative protein curvature.
- Error in BVM's approximation of boundary conditions η_b provides a measure of error in the BVM.
- This plot shows η_b decays with the truncation length N of the BVM's approximation of u.
- Finite element method [7] benchmark: G has error of $\lesssim 0.1\%$ when $\eta_b \leq 0.1\%$.
- These surfaces with colormaps were calculated by BVM; their colorbar is shown in the section below.

Simple analytical estimate of the bilayer thickness deformation energy due to protein of arbitrary shape

$$G_{\mathrm{analy}}\left(C(\theta)\right) = G_{\mathrm{cyl}}\left(R_{\mathrm{analy}} = \Gamma/2\pi\right) \longleftrightarrow C(\theta) \rightarrow R_{\mathrm{analy}}$$

$$G_{\mathrm{cyl}}(R) = \mathbf{i}K_b(2\pi R/\lambda)\frac{\left[(U/\lambda)K_1(\sqrt{\mathbf{i}}R/\lambda)\sqrt{\mathbf{i}} - U'K_0(\sqrt{\mathbf{i}}R/\lambda)\right]\left[(U/\lambda)K_1(\sqrt{-\mathbf{i}}R/\lambda)\sqrt{-\mathbf{i}} - U'K_0(\sqrt{-\mathbf{i}}R/\lambda)\right]}{K_0(\sqrt{-\mathbf{i}}R/\lambda)K_1(\sqrt{\mathbf{i}}R/\lambda)\sqrt{\mathbf{i}} - K_0(\sqrt{\mathbf{i}}R/\lambda)K_1(\sqrt{-\mathbf{i}}R/\lambda))\sqrt{-\mathbf{i}}}$$

- Analytical estimate replaces protein of any cross-section by protein of circular cross-section [9] with same circumference Γ and boundary conditions U and U'.

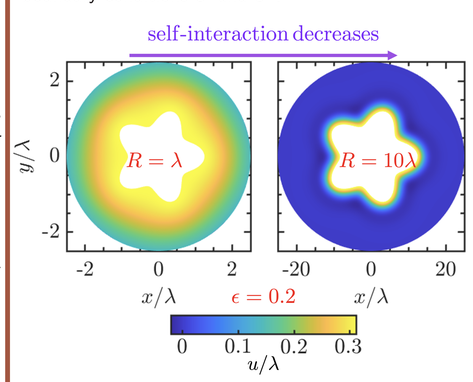

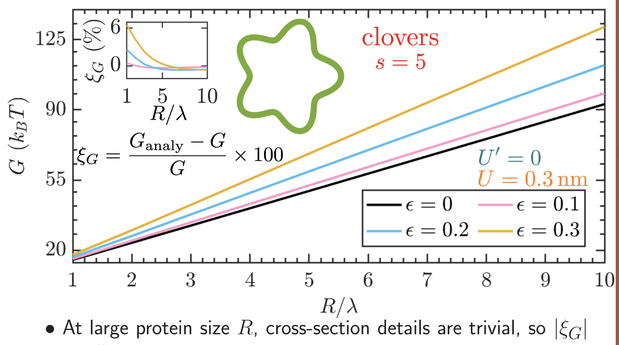

- Clover-leaf protein shapes have negative curvature which allow for overlap in bilayer thickness deformations, i.e. self-interactions.
- Due to deformation decay length λ, there is more overlap (self-interaction) at smaller R.
- At large protein size R, cross-section details are trivial, so $|\xi_G|$ is small.
- At smaller R, self-interactions, akin to interactions of pair proteins [3], can significantly impact G.
- Polygon protein shapes don't experience self-interactions so have $|\xi_G| < 1\%$, for $R \geq \lambda$.

Examining the relative stability of protein shapes

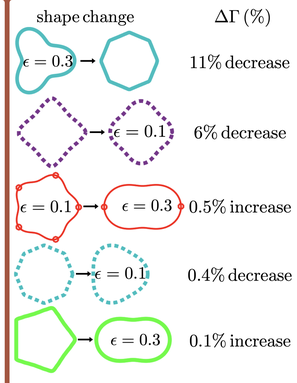

- We held protein cross-section area A and boundary conditions U and U' constant in transitions.

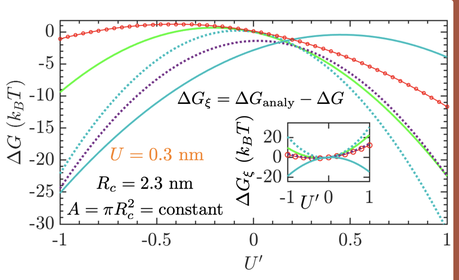

- Proteins of smaller cross-section circumference Γ tend to be more stable.
- When $\Delta\Gamma \approx 0$, proteins with weaker cross-section variations are more stable.
- ΔG_ξ show that $U' = 0$ minimizes importance of protein cross section details.

Structural co-factors may serve to destabilize protein oligomers

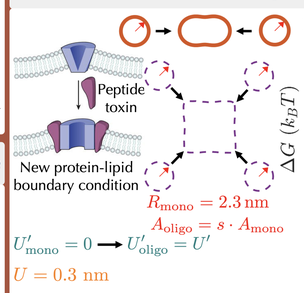

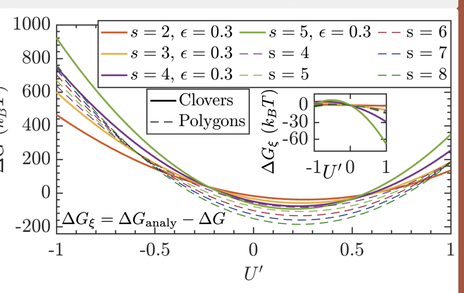

- Structural co-factors, i.e. tight binding lipids or peptides, can change boundary conditions [3].
- We assume monomers are cylindrical and identical and we ignore their interactions.
- We set oligomer cross-section area A_{oligo} to total cross-section area of monomers.
- $\Delta\Gamma << 0$, so oligomers more stable when $U'_{\mathrm{oligo}} \approx U'_{\mathrm{mono}} = 0$.
- Structural co-factors can serve to destabilize oligomers if they induce a large enough change in U'.
- ΔG_ξ show $\Delta G \approx \Delta G_{\mathrm{analy}}$, so oligomers' cross-section details tend not to significantly impact their stability.

Can bilayer mechanics account for the temperature sensing of cells?

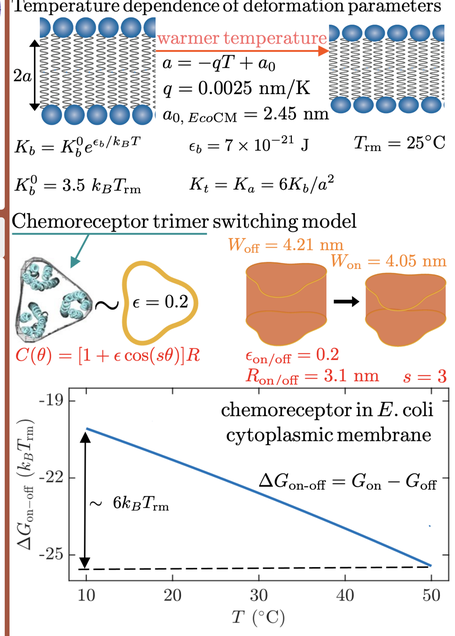

- $E.$ coli thermotax to warmer temperatures with some of the same chemoreceptors used to chemotax [10].
- Experimental measurements of the temperature dependence of DOPC bilayer mechanical properties [11] can be, roughly, adapted for $E.$ coli cytoplasmic membranes.
- Chemoreceptors [12] can be modeled as a button or switch with a 3-leaf clover cross-section [13].
- Bilayer thickness deformation contribution $\Delta G_{\mathrm{on-off}}$ to chemoreceptor activation energy decreases in warmer temperatures, with decreases on the order of chemoreceptor methylation energies ($\sim 1\ k_BT_{\mathrm{rm}}$ [14]).

Acknowledgements and References

This work was supported by the National Science Foundation Grant No. DMR-1554716 and C.D.A gratefully acknowledges support from a USC Graduate School DIA Fellowship. We give thanks to Dr. Osman Kahraman for his contributions on modeling the mechanism for the temperature sensing of cells, Dr. Fabien Pinaud for his suggestion to study protein oligomers, and Marco Olguin for his technical tips and support at USC CARC.

[1] Zhenfeng Liu et. al., *Nature*, **461**:120, 2009.
[2] Eduardo Perozo et. al., *Nature Structural Biology*, **9**:696, 2002.
[3] Rob Phillips et. al., *Nature*, **459**:379, 2009.
[4] Osman Kahraman et al., *Europhysics Letters*, **107**:48004, 2014.
[5] Olaf S. Andersen and Roger E. Koeppe II, *Annual Review of Biophysics and Biomolecular Structure*, **36**:107, 2007.
[6] H.W. Huang, *Biophysical Journal*, **50**:1061, 1986.
[7] Osman Kahraman et al., *Physical Review E*, **93**:042410, 2016.
[8] Alain Robert, *The American Mathematical Monthly*, **101**:420, 1994.
[9] Paul Wiggins and Rob Phillips, *Biophysical Journal*, **88**:880, 2005.
[10] Anja Paulick et. al., *eLife*, **6**:e26607, 2017.
[11] Jianjun Pan et. al., *Biophysical Journal*, **94**:117, 2008.
[12] Jun Liu et. al., *Proceedings of the National Academy of Sciences*, **109**:E1481, 2012.
[13] Christoph A. Haselwandter and Ned S. Wingreen, *PLoS Computational Biology*, **10**:e1003932, 2014.
[14] Thomas S. Shimizu et. al., *Molecular Systems Biology*, **6**:1, 2010.

calas@usc.edu